IN-02-TM

FINAL REPORT

1. AFOSR CONTRACT NUMBER: MIPR NO: 90-0012, 91-0007 and 92-0004

2. AFOSR PROJECT/TASK: 2307/A3

3. PERIOD COVERED BY REPORT: 1 October 1989 - 30 September 1992

4. TITLE OF PROPOSAL: Compressibility Effects on Dynamic Stall of Airfoils Undergoing Rapid Transient Pitching Motion

5. NAME OF INSTITUTION: Naval Postgraduate School

6. AUTHORS OF REPORT: M.S.Chandrasekhara and M.F.Platzer

7. LIST OF MANUSCRIPTS SUBMITTED OR PUBLISHED UNDER AFOSR SPONSORSHIP DURING THIS REPORTING PERIOD, INCLUDING JOURNAL REFERENCES:

See next page.

8. SCIENTIFIC PERSONNEL SUPPORTED BY THIS PROJECT:

The following personnel were partially supported by this project:

1. Prof. M.S.Chandrasekhara .
2. Prof. M.F.Platzer
3. Dr. L.W.Carr (cooperative participant) U.S.Army Aeroflightdynamics Directorate
4. Dr. S.Ahmed (MCAT Institute, Contractor to NASA Ames Research Center)
5. Dr. M.C. Wilder, (MCAT Institute, Contractor to NASA Ames Research Center)

M.S.Chandrasekhara
Code AA/CH
Department of Aeronautics and Astronautics
Naval Postgraduate School
Monterey, CA 93943

List of Publications

1. M.S.Chandrasekhara, L.W.Carr, and J.A.Ekaterinaris, "Interferometry and Computational Studies of an Oscillating Airfoil Compressible Dynamic Stall", presented at *The 5ᵗʰ Asian Congress of Fluid Mechanics*, Taejon City, Korea, Aug. 10-13, 1992.

2. N.Brock, M.S. Chandrasekhara, and L.W. Carr, "A Real Time Interferometry System for Unsteady Flow Measurements", IEEE Publication 91-CH3028-8, pp 423-430.

3. M.S.Chandrasekhara, S.Ahmed and L.W.Carr, "Schlieren Studies of Compressibility Effects on Dynamic Stall of Airfoils in Transient Pitching Motion", To appear in *Journal of Aircraft*.(**AIAA Paper 90-3038**).

Papers Published with Partial AFOSR Support

1. M.S.Chandrasekhara, and L.W. Carr, "Flow Visualization Studies of the Mach Number Effects on the Dynamic Stall of Oscillating Airfoils", *Journal of Aircraft*,Vol. 27, No. 6, pp. 516-522, 1990. (**AIAA Paper 89-0023**).

2. L.W.Carr, and M.S.Chandrasekhara, "A Study of Compressibility Effects on Dynamic Stall of Rapidly Pitching Airfoils", *Computer Physics Communications*, Elsevier Science Publishers, B.V., Vol 65, pp 62-68, 1991.

3. L.W.Carr, and M.S.Chandrasekhara, "Design and Development of a Compressible Dynamic Stall Facility", *Journal of Aircraft*, Vol 29, pp 314-318, 1992. (**AIAA Paper 89-0647**).

4. L.W.Carr, M.F.Platzer, M.S.Chandrasekhara, and J.A.Ekaterinaris, "Experimental and Computational Studies of Dynamic Stall" in *Numerical and Physical Aspects of Aerodynamic Flows IV*, Springer Verlag, Editor: T.Cebeci.

5. M.F.Platzer, M.S.Chandrasekhara, J.A.Ekaterinaris and L.W.Carr, "Dynamic Airfoil Investigations", presented at the *5ᵗʰ Symposium on Numerical and Physical Aspects of Aerodynamic Flows*, Jan. 13-15, 1992, Long Beach, CA.

6. M.S.Chandrasekhara and S.Ahmed, "Laser Velocimetry Measurements of Oscillating Airfoil Dynamic Stall Flow Field", **AIAA Paper 91-1799**, presented at the 22nd Fluid Dynamics, Plasma Dynamics and Lasers Conference, June 24-26, 1991, Honolulu, HI.

7. S.Ahmed and M.S.Chandrasekhara, "Reattachment Studies of an Oscillating Airfoil Dynamic Stall Flow Field", **AIAA Paper 91-3225**, presented at the 9th Applied Aerodynamics Conference, Baltimore, MD Sept. 23 - 25, 1991.

8. R.D.Vandyken and M.S.Chandrasekhara, "Leading Edge Velocity Field of an Oscillating Airfoil in Compressible Dynamic Stall", **AIAA Paper 92 - 0193**, presented at the AIAA 30th Aerospace Sciences Meeting, Jan. 6 - 9, 1992, Reno, NV.

9. L.W.Carr, M.S.Chandrasekhara and N.Brock, "A Quantitative Study of Unsteady Compressible Flow on an Oscillating Airfoil", **AIAA Paper 91-1683**, presented at the 22nd Fluid Dynamics, Plasma Dynamics and Lasers Conference, June 24-26, 1991, Honolulu, HI.

10. M.S.Chandrasekhara and R.D.VanDyken, "Velocity Measurements Around the Leading Edge of an Oscillating Airfoil Experiencing Dynamic Stall", presented at the 8th Symposium on Turbulent Shear Flows, Sep. 9-11, 1991, Münich, Germany.

11. L.W.Carr, M.S.Chandrasekhara, S.Ahmed and N.Brock, "A Study of Dynamic Stall Using Real-Time Interferometry", **AIAA Paper 91-0007**, presented at the AIAA 29th Aerospace Sciences Meeting, Reno, NV, January 1991.

Acknowledgements

1. Summary

A project to study the "Compressibility Effects on Dynamic Stall of Airfoils Undergoing Rapid Transient Pitching Motion" was funded by AFOSR in FY-90. The objective of the study was to obtain a better understanding of unsteady flow separation as encountered in dynamic stall of airfoils, under local compressibility conditions and eventually control it for useful gains on real flight systems.

The research was carried out in the Compressible Dynamic Stall Facility, *CDSF*, at the Fluid Mechanics Laboratory(FML) of NASA Ames Research Center. The facility can produce realistic nondimensional pitch rates experienced by fighter aircraft, which on model scale could be as high as $3600^0/sec$. Nonintrusive optical techniques were used for the measurements. The highlight of the effort was the development of a new real time interferometry method known as *Point Diffraction Interferometry - PDI*, for use in unsteady separated flows. This can yield instantaneous flow field density information (and hence pressure distributions in isentropic flows) over the airfoil. A key finding is that the dynamic stall vortex forms just as the airfoil leading edge separation bubble opens-up. A major result is the observation and quantification of multiple shocks over the airfoil near the leading edge. A quantitative analysis of the PDI images shows that pitching airfoils produce larger suction peaks than steady airfoils at the same Mach number prior to stall. The peak suction level reached just before stall develops is *the same at all unsteady rates* and decreases with increase in Mach number. The suction is lost once the dynamic stall vortex or vortical structure begins to convect.

Based on the knowledge gained from this preliminary analysis of the data, efforts to control dynamic stall were initiated. The focus of this work was to arrive at a dynamically changing leading edge shape that produces only 'acceptable' airfoil pressure distributions over a large angle of attack range.

2. Introduction

Dynamic stall is an important problem and of particular interest to aircraft execut-

ing rapid maneuvers. The production of increased lift and stall delay during a transient maneuver could be effectively used to enhance the agility of fighter aircraft, provided the effect could be sustained for the duration of the maneuver. This requires a careful control of the process which is extremely complex[1,2] and depends on several factors such as Mach number, Reynolds number, pitch rate, airfoil geometry - leading edge shape - in particular, transition etc. Among these, the compressibility effects (Mach number), leading edge boundary layer transition and leading edge shape (pressure distribution) play a more critical role in altering the process. Compressibility effects set in at a very low free stream Mach number - 0.2 -0.3(McCroskey[1], Chandrasekhara et al[3], Chandrasekhara and Carr[4]), and can cause premature stall. Production of shocks[3] over the airfoil and their interaction with the local boundary layer are partly responsible for this. However, the development of the leading edge adverse pressure gradient to the critical value at which flow separation occurs, at a lower angle of attack, is the main reason for the premature stall observed under compressibility conditions.

The research effort described was aimed at understanding the underlying physical processes during the occurrence of dynamic stall of a 3in. chord NACA 0012 airfoil pitching transiently at rates of up to $3600^0/sec$ in a free stream flow ranging from M = 0.2 - 0.45. A new nonintrusive optical flow measurement technique referred to as Point Diffraction Interferometry was developed with the funding to obtain real time quantitative flow field information. The dynamic motion of the airfoil at rapid rates precluded use of other conventional measurement methods. The report describes the results of the effort.

3. Experimental Facility and Technique

3.1. The Facility

The experiments were performed in the Compressible Dynamic Stall Facility at NASA Ames Research Center. The CDSF[5] was established for conducting dynamic stall research in the FML. This facility is specifically designed for study of dynamic stall over a range of Mach numbers, using nonintrusive optical flow diagnostic techniques. It is operated as a part of the indraft tunnel complex at the FML. The CDSF is unique in that the airfoil is

6

supported between two 1in. thick optical quality glass windows by pins that are smaller than the local airfoil thickness. Thus, the entire flow field including the airfoil surfaces can be viewed unobstructed by any support mechanism. This enables the study of the flow at the surface near the leading edge, where the dynamic stall vortex forms, as well as the flow field away from the airfoil.

The rapid ramp-type pitching motion of the airfoil was produced by a hydraulic drive located on top of the test section. It can pitch an airfoil at constant pitch rates and is shown in Figure 1.

The specifications of the hydraulic drive are as follows:

angle of attack, α:	0-60°
pitch rate, $\dot{\alpha}$:	0-3600 ^{o}/sec
maximum acceleration rate:	600,000 $^o/sec^2$
change in α during acceleration:	$\leq$6° of pitch
minimum acceleration time:	4 ms
free stream Mach number:	0.1-0.5
airfoil chord:	3.0 in.
Reynolds number:	180,000 - 840,000

The pitch rate of 3600 ^{o}/sec on a 3in. chord airfoil corresponds to a 90°/sec pitching of a 10 ft. chord airplane wing at any given Mach number; thus, the rates obtainable from the design are directly applicable to flight conditions. In order to limit or isolate the effects of transients on separation, the change in angle of attack during acceleration and the acceleration time itself were limited to less than 6° and 4 ms, respectively. To properly simulate a maneuver, an angle of attack range of 0 - 60° was selected. To provide for reasonable experiment times, the facility has a recycle time of 2 seconds (30 runs/minute). The system uses both the airfoil position and velocity information in its feed back loops to properly perform any required maneuver which can be selected through software. The complete details of the final design are presented in Chandrasekhara and Carr[6].

The airfoil position was read by a digital optical encoder, whose output was input to the digital I/O board of a microVAX II Work Station and timed with its internal clock.

Figure 2 shows an example of the actual rates obtained, including the variation of the angle of attack during the various parts of the pitch-up motion in an experiment. It is clear that the airfoil pitches through its static stall angle at a constant rate of change of angle of attack. For the highest rate, the motion is completed in 15 ms, beyond which the system can be seen to be settling down (at the highest angle). All the tests were limited to the linear range.

Since its original design, changes were made to the drive system to incorporate additional safety features and augment the protective features of the drive. These include installation of pressure gages to show the pressure in the system, pressure relief valves to bypass the flow directly to the tank - a precaution needed to mitigate the strong water hammer effects felt when the system was suddenly depressurized, adding new plumbing to control the pressure in the hydraulic accumulator during each pitch-up, electrical system modifications that de-energize the solenoid valve and 'dump' the hydraulic line pressure, etc. Since the response of the feed back system would be altered by these components, a new system calibration was performed after tuning the feed back system properly to ensure stable operation of the system through the envelope of the experimental conditions.

3.2. Instrumentation and Techniques

The CDSF is equipped with a wide range of nonintrusive optical flow diagnostic instrumentation such as stroboscopic schlieren, laser Doppler velocimetry, and point diffraction interferometry systems. Only the schlieren and the interferometry systems are discussed in this report.

A. Stroboscopic schlieren studies

A standard mirror based schlieren system was set up in a 'Z' type configuration with a xenon arc lamp light source located at the focal length(10 ft.) of one of the mirrors. The beam passing through the test section was focused on to a vertical knife edge and imaging optics. The light source was triggered externally at the desired phase angles by an electronic circuit which compared the chosen phase angle of oscillation and the encoder

data from the drive system and produced a TTL pulse when a match occurred. No delays were found to be present between the events of matching the phase angle and the light flashing.

B. Interferometry studies

As stated earlier, the quantitative flow field density information was obtained using PDI. The PDI system used a CW/pulsed pumped Nd-YAG laser light source, with its beam expanded to 6in. to fill the entire field of view in the standard Z-type schlieren configuration. The optics were aligned to minimize astigmatism. A predeveloped, partially transmitting photographic plate was placed at the location of the knife edge as the PDI plate. Imaging optics were set up further downstream along the beam path for recording the flow. In operation, a pin hole was created *in situ* in the photographic plate with no flow in the test section. This acted as a point diffractor for the reference beam. Light deflected by the flow density changes (signal beam) focused to a slightly different spot, passed through the partially transmitting photographic plate and interfered with light passing through the pin-hole (which was the reference beam) to produce real time interference images, which were captured on Polaroid film. Fig. 3 shows a schematic of the final system used.

Several different PDI plates were tried in an effort to improve the quality of the interferograms obtained. Some of these were: a green line filter, an unexposed holographic film, a predeveloped holographic plate etc. The trials showed that the best performance was obtained from a plate with an optical density of about 1.0. However, as is well known, film development is a function of several parameters and thus, trial and error is still involved. A measurement of the plate optical density is a good indication of the performance that can be obtained.

One of the key parameters affecting the results of the technique is the size of the spot used as the point diffractor. A study to establish the sensitivity of the image quality and accuracy with respect to the spot size showed that spots of 50-80 μm diameter gave acceptable results over the whole flow field, including the dense region (with high frequency fringes) near the leading edge. These and other details have been documented in Ref. 7.

9

Ref. 7 and 8 describe more details of the technique and its implementation in the CDSF.

C. Fringe Analysis and Image Processing

A review of the available options for fringe analysis and image processing showed that the standard packages are very limited and almost exclusively, application specific. Thus, the task of developing a software package was undertaken in stages. In the present version, the package runs in a semi-automatic mode. It reads a digitized (256 gray level) interferogram and overlays the airfoil on the image. In addition, two slightly larger airfoils are also drawn. The user interactively picks the intersection of the fringes with the airfoil upper and lower surfaces separately. When the fringe density is high, it permits the user to go into the 'off-body' mode and pick fringes along a line parallel to and away from the airfoil surface (on one of the larger airfoils) where the fringes are farther apart. These are then transferred to the airfoil surface. Typically, the fringes near the leading edge region are very dense in the flow field being studied owing to the very large local density gradients. Optical noise introduced by the shadowgraph effect in this region lowers the contrast, making it an ideal location where the off-body mode needs to be invoked. The package provides an output data file containing the various physical variables, using isentropic flow relations in a format suitable for the FML/NASA ARC standard QPLOT graphics package. Presently, the data is being processed on an IRIS 4000 Series Work Station and it takes about 3 - 5 minutes per image for processing.

4. Results and Discussion

The results are presented in the form of schlieren pictures, PDI images and plots of data retrieved from these flow images. The schlieren results are described in ref. 3 and are simply reproduced here for completeness.

4.1. Effect of Mach Number

Fig. 4 compares the schlieren pictures at different Mach numbers for $\alpha^+ = 0.03$ and $\alpha = 17^0$. It can be seen that for $M \leq 0.3$, the vortex is at about 50% chord location.

In addition, the vertical extent of the flow is nearly the same for M = 0.2, 0.25 and 0.3. However, for $M \geq 0.3$, the dynamic stall vortex moves successively closer to the trailing edge and the flow scales can be seen to have increased as well. Movement of the vortex downstream indicates that the flow is approaching the deep stall state and thus, it is clear from the figure that as the Mach number is increased above 0.3, deep stall occurs at progressively lower angles of attack.

Fig. 5a shows the effect of Mach number on dynamic stall for a pitch rate, $\alpha^+ = 0.025$, and the corresponding results for $\alpha^+ = 0.035$ are shown in Fig. 5b. Plotted in it are the successive locations of the center of the dynamic stall vortex as a function of the instantaneous angle of attack at different Mach numbers. It can be seen in both figures that the vortex appears at lower angles of attack as the Mach number increases. This also leads to the result that the vortex moves past the trailing edge at lower angles of attack for higher Mach numbers, causing deep dynamic stall to occur earlier in the pitch-up motion. Significant decrease in the angle of attack occurs for the same x/c location for $M \geq 0.3$ and thus, M = 0.3 can be considered to be the limit when compressibility effects set in. Consider for example Fig. 5a, for x/c ≈ 0.6, the center of the vortex is at $\alpha = 16.5^0$ for M = 0.3, and $\alpha = 14^0$ for M = 0.45. Similarly, in Fig. 5b, the vortex is at 60% chord location at $\alpha = 19^0$ for M = 0.3; at M = 0.4, the corresponding angle of attack = 17.2^0. Similar results were obtained at other pitch rates.

4.2. Effect of Pitch Rate

Fig. 6a through 6d show the vortex center locations over the airfoil plotted as a function of the angle of attack at different pitch rates for M = 0.2, 0.35, 0.4 and 0.45 respectively. It can be seen in all the figures that the vortex is retained on the surface of the airfoil to higher angles of attack as the pitch rate is increased. The trend is monotonic with increasing pitch rate. For example at M = 0.45, the vortex is on the surface even at $\alpha = 18^0$ at $\alpha^+ = 0.03$, whereas the static stall angle for this case is $\approx 9.5^0$ as determined from the schlieren images. For $\alpha^+ = 0.020$, deep dynamic stall occurs at $\alpha = 15.5^0$. For M = 0.35, the deep stall angle is $\approx 23^0$ for $\alpha^+ = 0.04$, and the static stall angle is 11.6^0.

4.3. Leading Edge Supersonic Flow

There has been discussion for a long time about the possibility of a shock developing in the leading edge flow. Fig. 7 provides conclusive proof that a shock, in fact, multiple shocks form in the flow. It shows a schlieren picture of the flow at $M = 0.45$, $\alpha = 12.6^0$ at $\alpha^+ = 0.0313$ and a PDI image for the same conditions. The latter actually allows quantification of the flow. A simple fringe counting shows that the local Mach number ahead of the shock is greater than 1.0 and at the foot of the shock, it is about 1.2. Although the flow is only weakly supersonic, the shock causes the leading edge laminar boundary layer to separate. This separated free shear layer develops a waviness, which causes the flow downstream of the shock to go through a series of accelerations and decelerations. As the flow negotiates the crests and valleys of this wavy shear layer, expansion waves and compression waves develop, causing a series of shocks. The last shock in the series appears to be the strongest and the flow becomes subsonic downstream. Further analysis of this interesting basic flow is ongoing. The shocks are repeatable, and have been found to be present over an angle of attack range of about one degree.

4.4. Separation Bubble and Dynamic Stall

Fig. 8a is a point diffraction interferogram of the flow at $M = 0.3$, $\alpha = 12^0$ and $\alpha^+ = 0.03$. This image reveals some important features of the flow. Firstly, the dark fringe on the lower surface slightly aft of the leading edge is the stagnation point fringe. The suction pressure developed by the airfoil causes the local flow to accelerate, resulting in strong density changes, which is seen in the figure as a concentration of high frequency fringes. The close spacing of the fringes also means that the flow gradients are very high. In fact, 21 dark fringes are present in 1 millimeter in this image, indicating that the local Mach number is 0.71 and the local pressure coefficient is -3.75 at $x/c = 0.01$. Downstream of this the steep adverse pressure gradient region where the classic laminar flow separation occurs. The separated shear layer reattaches after it transitions into a turbulent layer, forming a bubble. The accompanying pressure distribution obtained by processing the image using the fringe analysis software developed is plotted in Fig. 8b. It shows the

suction peak, the drop in suction due to the adverse pressure following it and the laminar separation bubble, the later is indicated by the plateau in the distribution. Downstream of the plateau, the pressure gradually recovers to the free stream value. When several such pictures were analyzed, it was found that the nondimensional pressure gradient $\left(\frac{dC_p}{d(\frac{x}{c})} \right)$ at which the bubble opens up is about 100. As the shear layer moves outwards, the dynamic stall vortex forms. During this stage, the airfoil continues to develop additional suction (since the shear layer is still attached at the leading edge). However, once the vortex grows and begins to convect, the suction drops. Interestingly, during the convection process, the pressure distribution flattens out, leading to continued production of lift. These details are discussed further in ref. 9. Only sample pressures distributions are shown in Fig. 9 for angles of attack ranging from 11 - 15 degrees.

4.5. Leading Edge Flow Development *vs.* Unsteadiness

The maximum suction pressure attained in the flow just before the vortex formed and became discernible in the PDI pictures was estimated by fringe counting. Its variation with the pitch rate is shown in Fig. 10[9]. Included in it are the steady flow values when stall occurred. A significant result is the near constancy of the $C_{P_{min}}$ at a given Mach number for all unsteady flow cases plotted. The values are always higher than the steady flow levels, clearly indicating the fact that transient pitching of the airfoil keeps the fluid attached enabling the airfoil to develop larger suction. Further, since the airfoil reaches a higher angle of attack before the vortex forms, stall delay is concomitant with the pitching process. It can be inferred from this that the leading edge pressure distribution is modified considerably by pitching the airfoil. The striking result in the figure is the strong dependence of the peak suction pressure coefficient on Mach number, decreasing monotonically with increasing Mach number.

Fig. 11 compares the development of the peak suction pressure coefficient with angle of attack for M = 0.4 at different degrees of unsteadiness. It is evident that the pressure development lags that of steady flow by a few degrees, depending on the rate of pitching. In addition, the unsteady flow also can reach a higher suction peak of -4.5 (and hence

13

higher lift) as opposed to the steady flow value of about -3.0. The peak remains high as the vortex forms and grows, but once vortex convection starts, it begins to drop. The vortex formation and growth occurs over an angle of attack range of about half-a-degree.

4.6. Control of Dynamic Stall

The PDI studies have revealed that the leading edge pressure distribution development is delayed in unsteady flows. To use dynamic stall benefits in aircraft systems, this delay needs to be sustained and even, increased further. Since the dynamic stall vortex occurrence correlates with the $C_{p_{min}}$ values over the leading edge (presumably the level at which the critical adverse pressure gradient for stall is encountered downstream) a possibility exists that if the pressure distribution is altered suitably, stall control could be achieved. Towards this goal, a flexible leading edge over an airfoil offers excellent potential, since the airfoil geometry could be instantaneously modified to produce a favorable pressure distribution *always*. A material developed and patented at NASA ARC has been found to have the necessary properties for this attempt. This material is a sheet of plastic, in which are embedded two strips of a conducting material. When subjected to a like charge, the repulsive force between the two strips produces sizeable surface deformation. Such a device is now being used to de-ice aircraft wings.

In the current application, the idea is to replace the airfoil leading edge with this material, apply a controlled voltage to it and produce a dynamically deformable leading edge (DDLE). An existing airfoil made from this sheet was subjected to different voltages. The rapid surface deformation cycle that resulted lasted about 3 milliseconds. Images of the surface were recorded with a high speed IMA-CON camera (at rates of up to 25,000 frames/sec). The camera imaged up to 16 frames at the selected rate. The challenge was to identify the portion of the surface that was being studied and illuminate it properly for good photographs to be obtained. An orthogonal grid of retro-reflecting tape glued to the airfoil and lit by strobe lights provided this information. The camera and the strobe lights were triggered by the same pulse generator driving the leading edge deformation circuit. The camera/strobe circuit incorporated a controllable delay so that any desired portion of

14

the deformation cycle could be recorded. Fig. 12 shows the schematic of the arrangement used. The resulting images were digitized and processed on an IRIS Work Station, using software developed in-house. The deflections were measured from a stationary reference. A sample plot of the deformation is shown in Fig. 13, where a section of the surface is plotted at three instants of time.

The deformation of the strips used was found to be three dimensional which is obviously unacceptable for dynamic stall control. Design effort is now underway to achieve a two-dimensional surface deflection through a deformation cycle. The aerodynamic behavior of the airfoil will then be examined to determine its effectiveness in overcoming both static and dynamic stall.

5. Concluding Remarks

A comprehensive study of dynamic stall of a transiently pitching airfoil has been conducted. It has shown that:

1. Compressibility effects set in at a Mach number of 0.3.

2. Dynamic stall arises out of the bursting of a laminar separation bubble near the leading edge on the upper surface of the airfoil.

3. Multiple shocks form over the airfoil at M = 0.4 and above, for certain angles of attack. The associated fluid flow interactions are very complicated.

4. The suction pressure coefficient is a function of the Mach number only and decreases with increasing Mach number.

5. The delay of stall is brought about by a delay in the development of the leading edge pressure distribution, when compared to steady flow under the same conditions. Increasing unsteadiness increases the delay.

6. The correlation between the airfoil peak suction pressure coefficient and dynamic stall occurrence leads to stall control ideas using adaptive geometries, which are being attempted. The challenge is to form a flexible leading edge airfoil that can deflect only in two dimensions. The effects of changing leading edge geometry on fluid flow still needs to be investigated.

6. References

1. W.J.McCroskey, "The Phenomenon of Dynamic Stall", NASA TM 81264, March 1981.

2. L.W.Carr, "Progress in Analysis and Prediction of Dynamic Stall", *Journal of Aircraft*, Vol. 2, No. 1, 1988, pp. 6-17.

3. M.S.Chandrasekhara, S.Ahmed and L.W.Carr, "Schlieren Studies of Compressibility Effects on Dynamic Stall of Airfoils in Transient Pitching Motion", To appear in *Journal of Aircraft*.(**AIAA Paper 90-3038**).

4. M.S.Chandrasekhara, and L.W. Carr, "Flow Visualization Studies of the Mach Number Effects on the Dynamic Stall of Oscillating Airfoils", *Journal of Aircraft*,Vol. 27, No. 6, pp. 516-522, 1990. (**AIAA Paper 89-0023**).

5. L.W.Carr, and M.S.Chandrasekhara, "Design and Development of a Compressible Dynamic Stall Facility", *Journal of Aircraft*, Vol 29, pp 314-318, 1992. (**AIAA Paper 89-0647**).

6. Chandrasekhara, M.S. and Carr, L.W., "Design and Development of a Facility for Compressible Dynamic Stall Studies of a Rapidly Pitching Airfoil", *ICIASF'89 RECORD* IEEE Publication 89-CH2762-3, pp. 29-37.

7. N.Brock, M.S. Chandrasekhara, and L.W. Carr, "A Real Time Interferometry System for Unsteady Flow Measurements", *ICIASF'91 RECORD*, IEEE Publication 91-CH3028-8, pp 423-430.

8. L.W.Carr, M.S.Chandrasekhara, S.Ahmed and N.Brock, "A Study of Dynamic Stall Using Real-Time Interferometry", **AIAA Paper 91-0007**, presented at the AIAA 29th Aerospace Sciences Meeting, Reno, NV, January 1991.

9. M.S.Chandrasekhara, L.W.Carr and M.C.Wilder, "Interferometric Investigations of Compressible Dynamic Stall Over a Transiently Pitching Airfoil", **AIAA Paper 93-**

0211, to be presented at the 31st Aerospace Sciences Meeting, Reno, NV, Jan. 11-14, 1993.
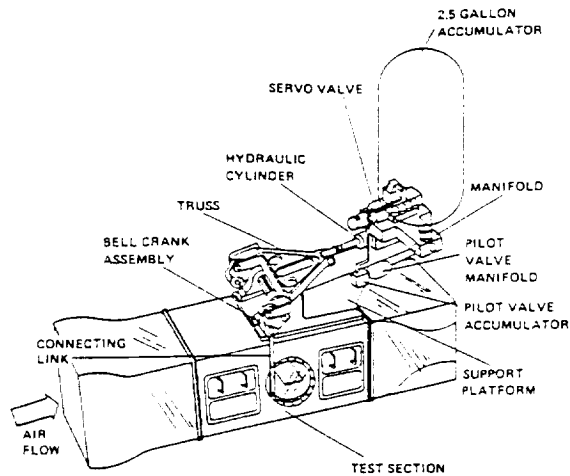
Fig. 1. Diagram of the In-draft Wind Tunnel with the Constant Pitch Rate Mechanism
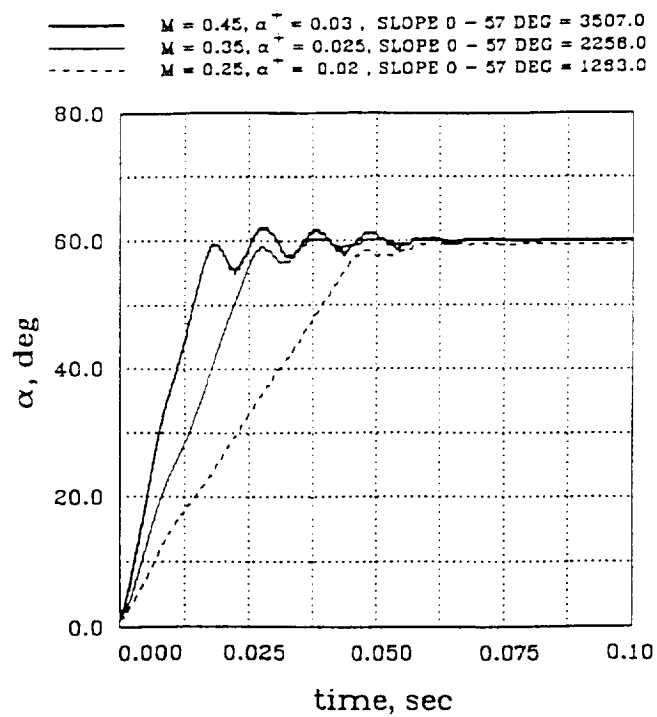

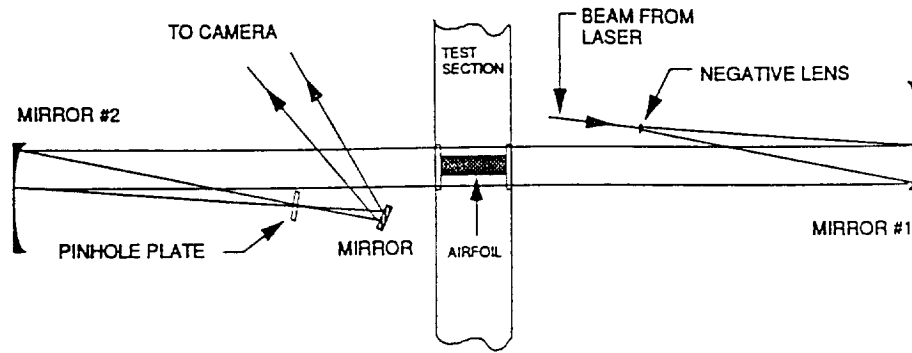Fig. 2. Time-history of Ramp for Sample Test Conditions

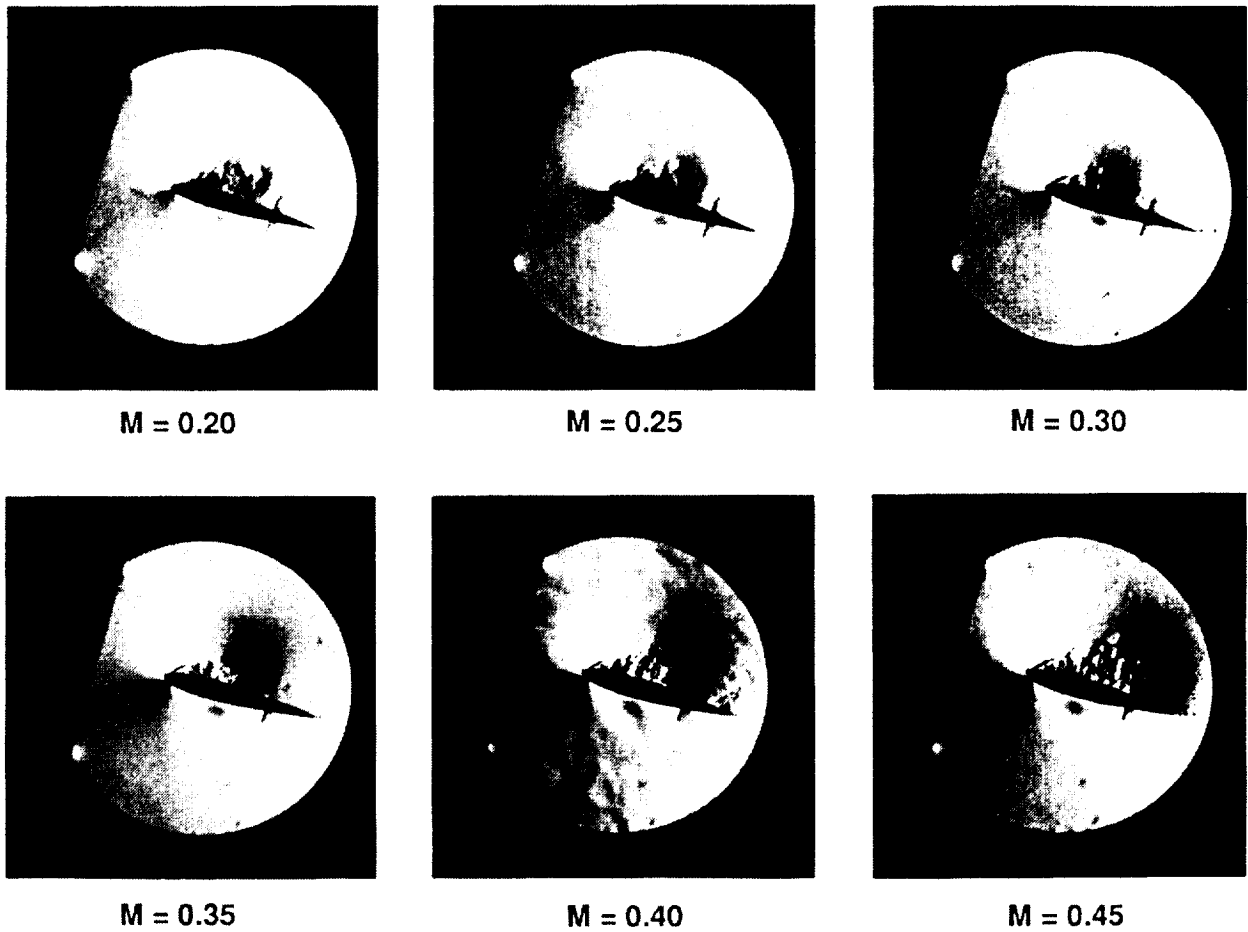Fig. 3. Schematic of the Point Diffraction Interferometer.

M = 0.20 **M = 0.25** **M = 0.30**

M = 0.35 **M = 0.40** **M = 0.45**

Fig. 4. Effect of Mach Number on Dynamic Stall of a Rapidly Pitching Airfoil: $\alpha^+ = 0.03, \alpha = 17\text{deg}$.

19
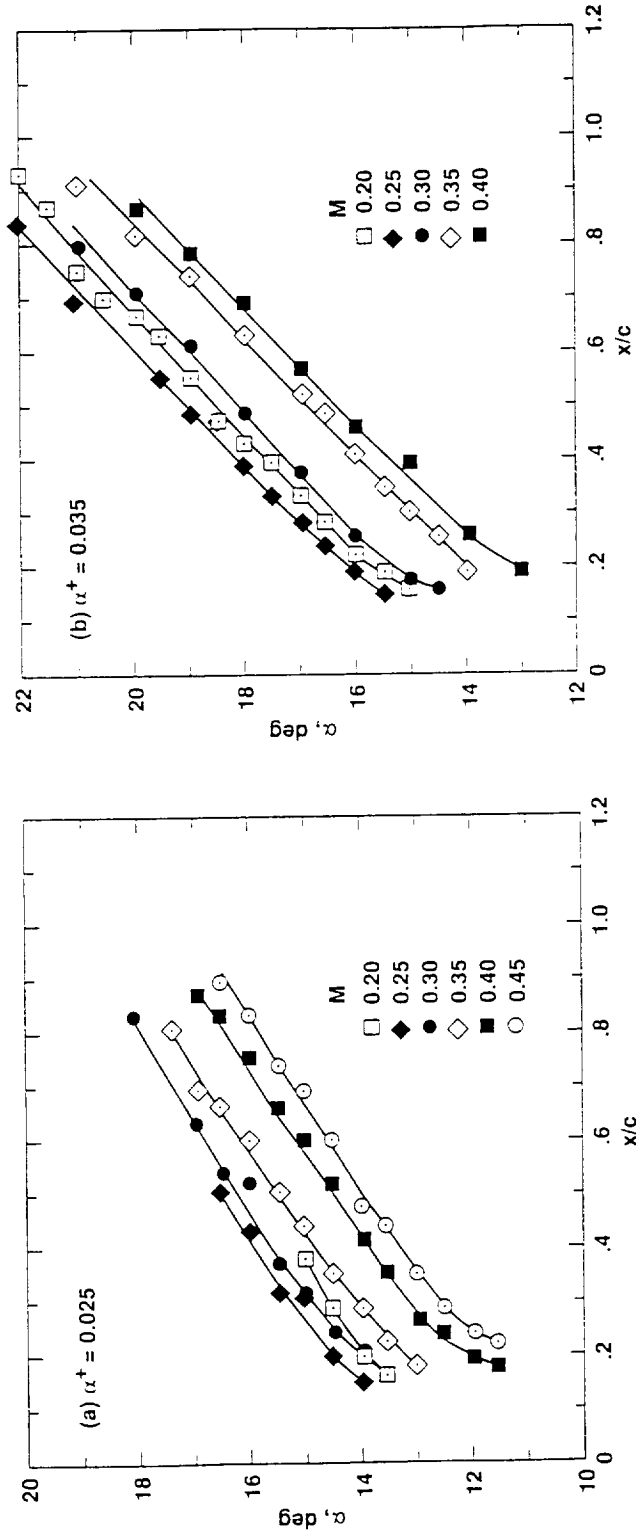
Fig. 5. Quantitative Effects of Mach Number on Dynamic Stall Vortex Location: (a) $\alpha^+ = 0.025$, (b) $\alpha^+ = 0.035$.
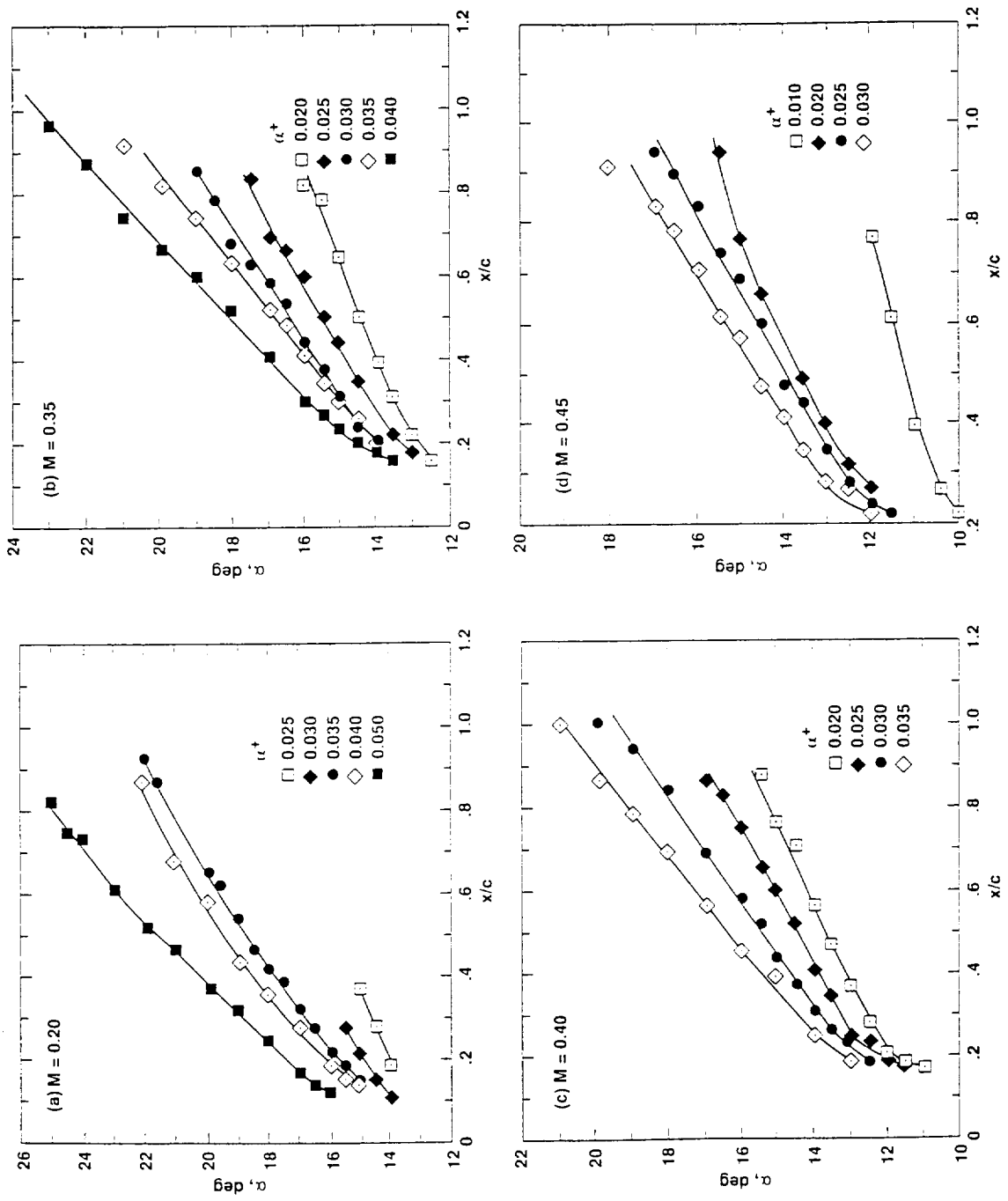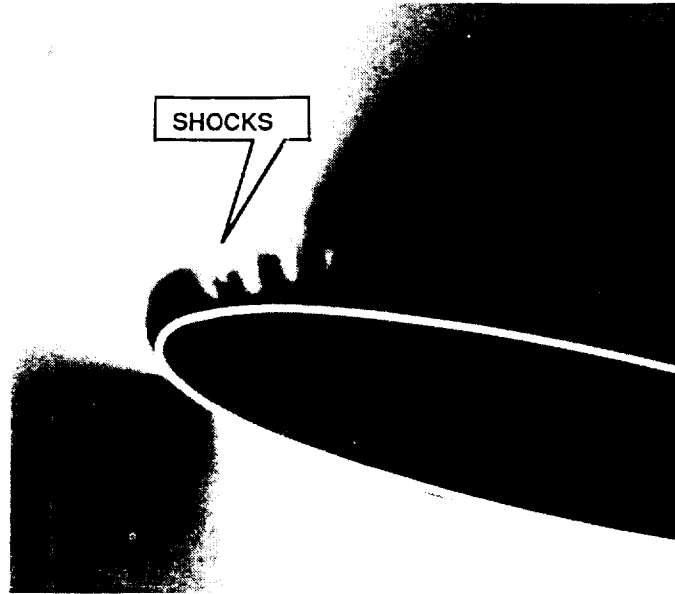
20

Fig. 6. Quantitative Effects of Pitch Rate on Dynamic Stall Vortex Location: (a) M = 0.2, (b) M = 0.35, (c) M = 0.40, (d) M = 0.45.

(a) Schlieren Picture

(b) Point Diffraction Interferogram
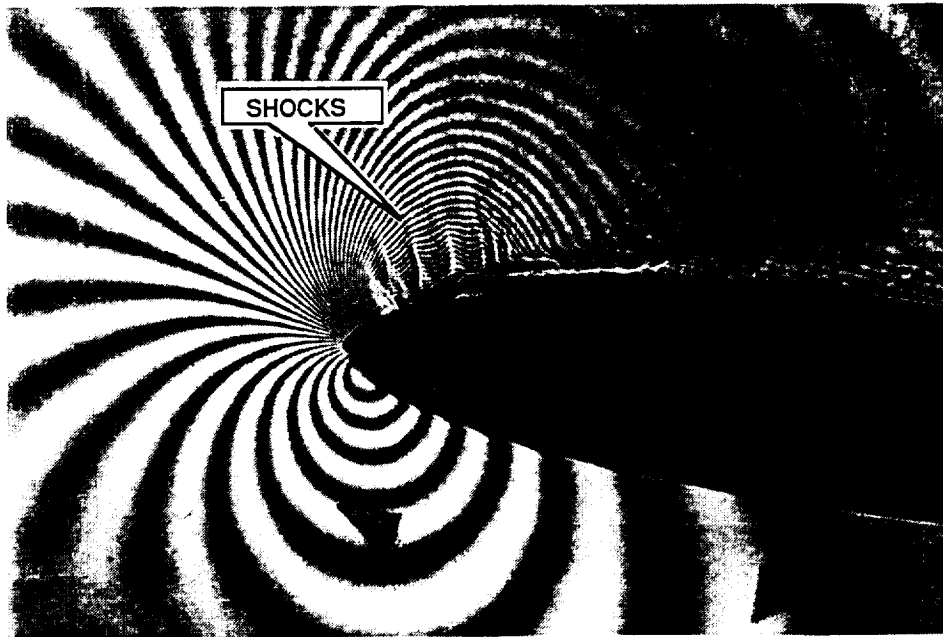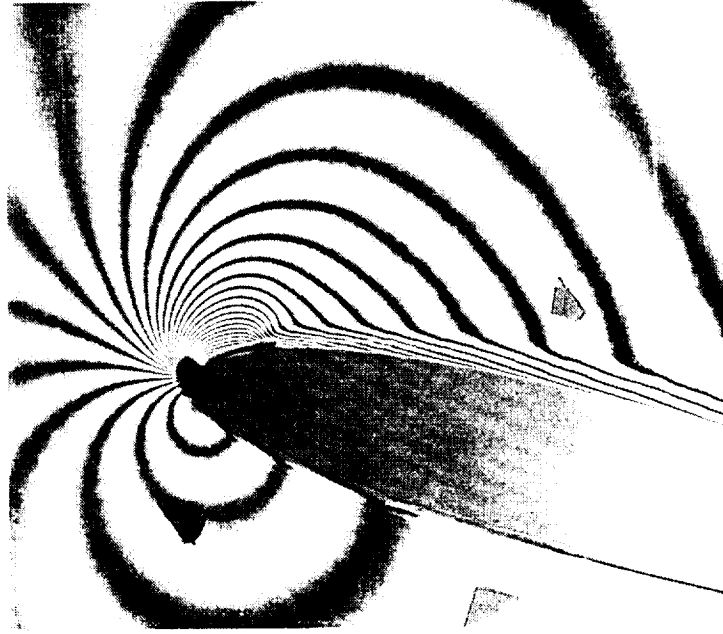

Fig. 7. Multiple Shocks on a Rapidly Pitching Airfoil: M = 0.45, $\alpha^+ = 0.0313$, $\alpha = 12.6^0$.

(a) Interferogram

(b) Pressure Distribution

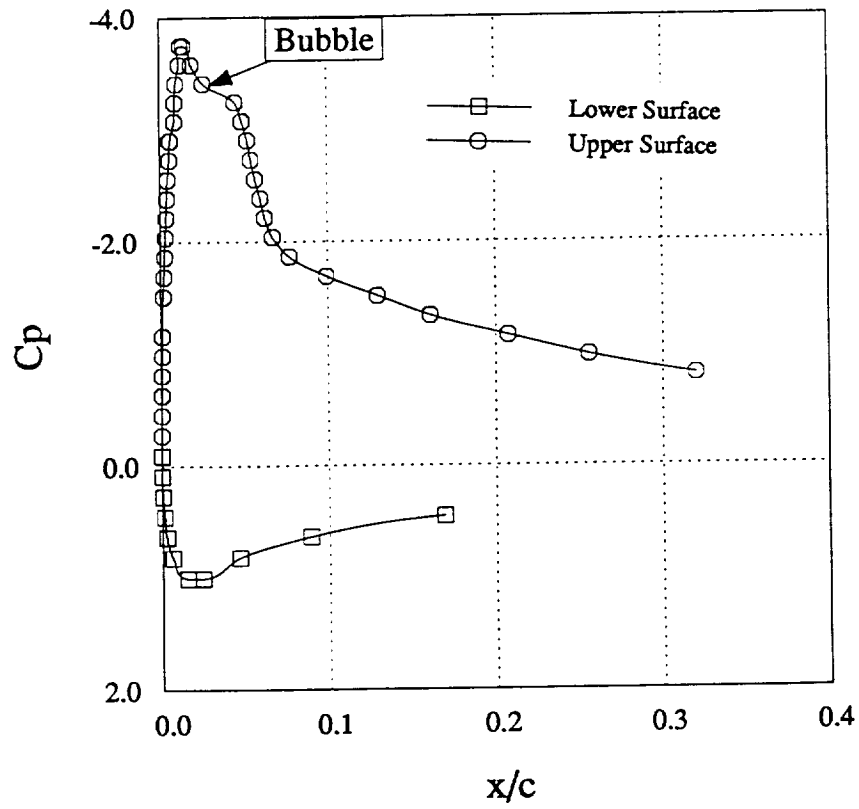Fig. 8. Flow Over a Transiently Pitching Airfoil: $M = 0.03$, $\alpha = 12^0$, $\alpha^+ = 0.03$.

23

Pressure Distributions Over Transiently Pitching Airfoil
M = 0.3, α^+ = 0.04

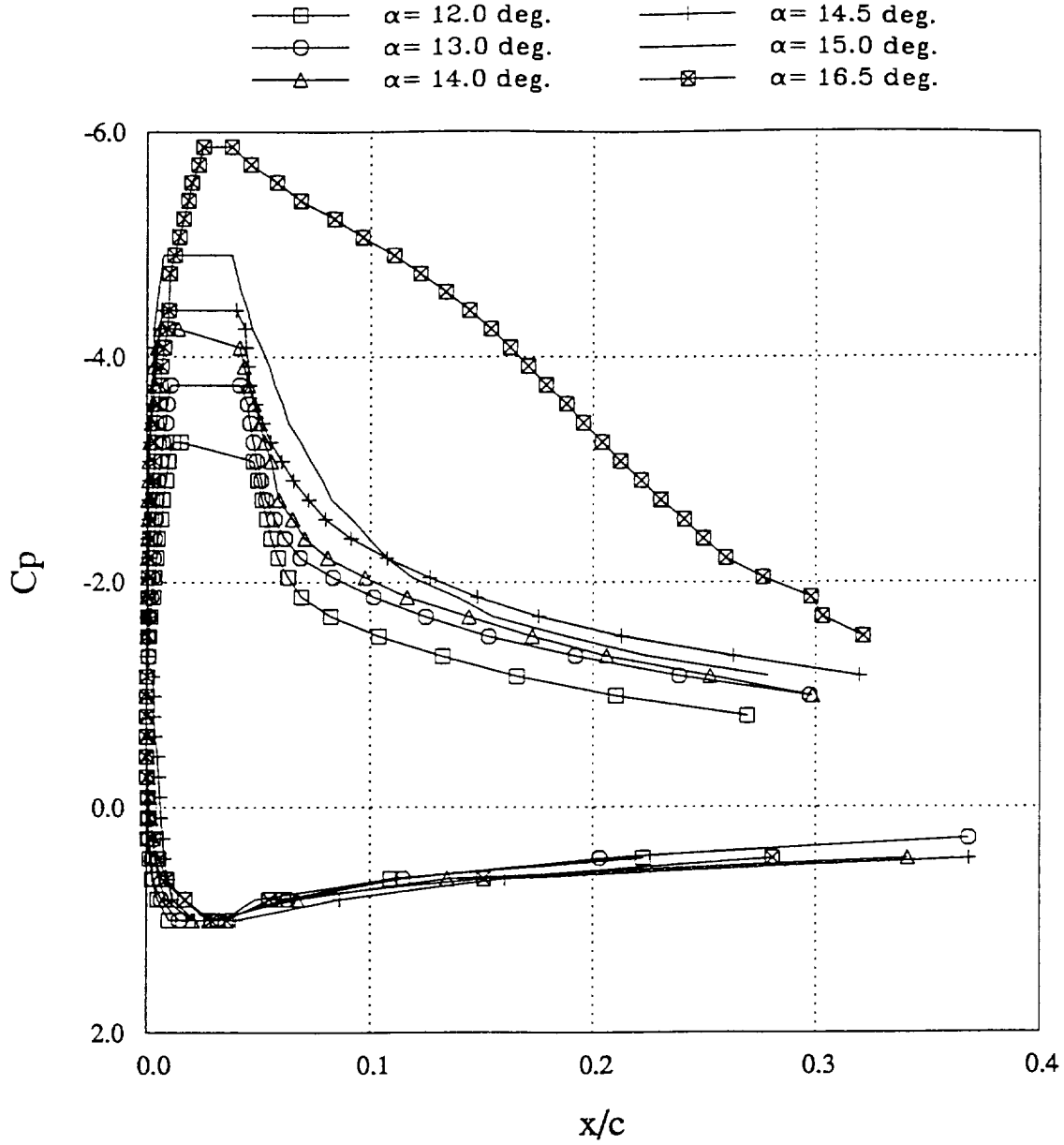|		
—□—	α= 12.0 deg.	—+— α= 14.5 deg.
—○—	α= 13.0 deg.	—— α= 15.0 deg.
—△—	α= 14.0 deg.	—⊠— α= 16.5 deg.

Fig. 9. Pressure Distributions Over a Transiently Pitching Airfoil During Dynamic Stall Onset: M = 0.3, α^+ = 0.04.

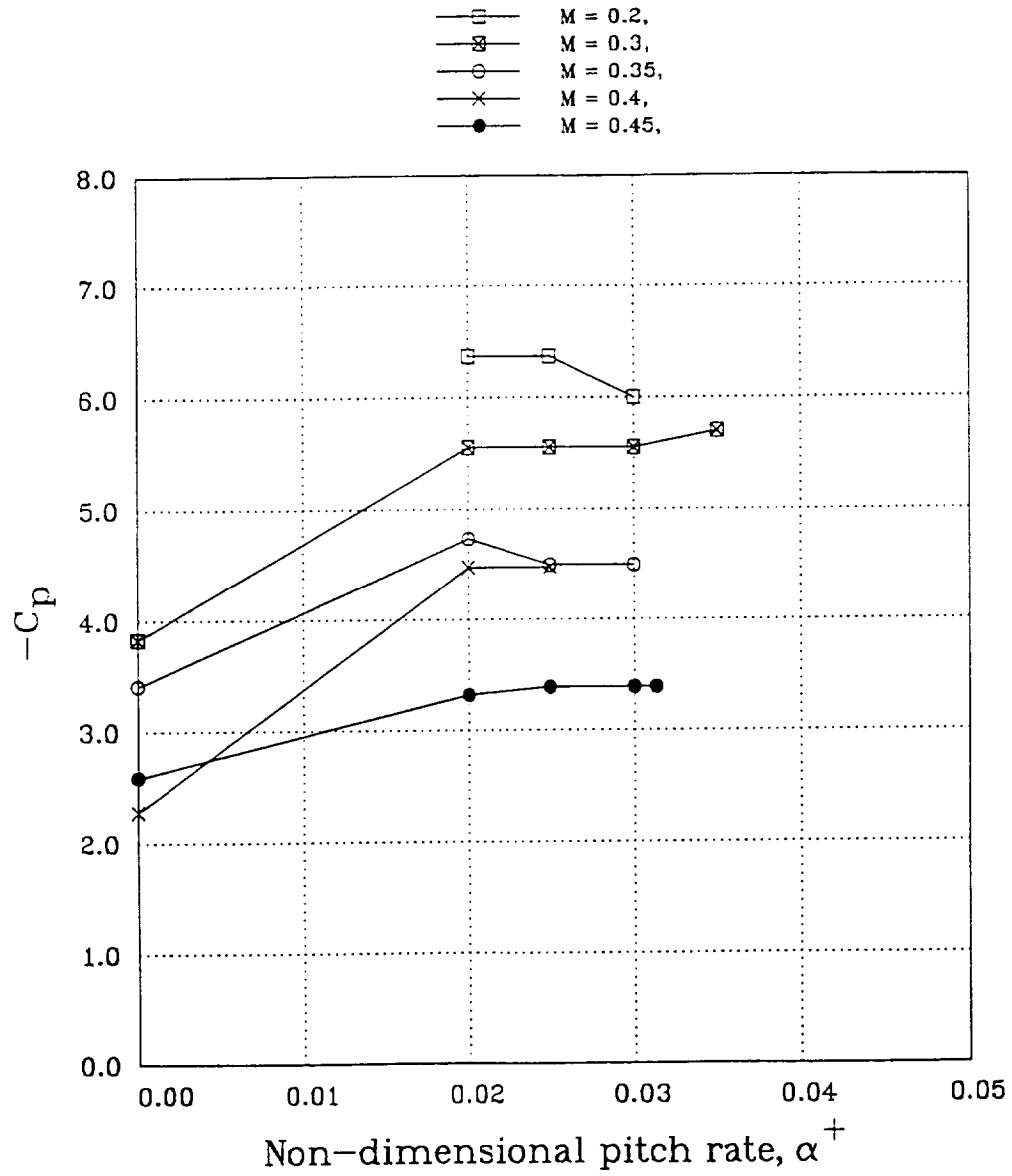# Pressure Coefficients at Stall Vortex Formation VS α^+

M = 0.2,
M = 0.3,
M = 0.35,
M = 0.4,
M = 0.45,

Fig. 10. Effect of Mach Number on Peak Suction Pressure Coefficients Over a Transiently Pitching Airfoil.

Pressure Coefficients Vs Angle of Attack, $M_\infty = 0.40$

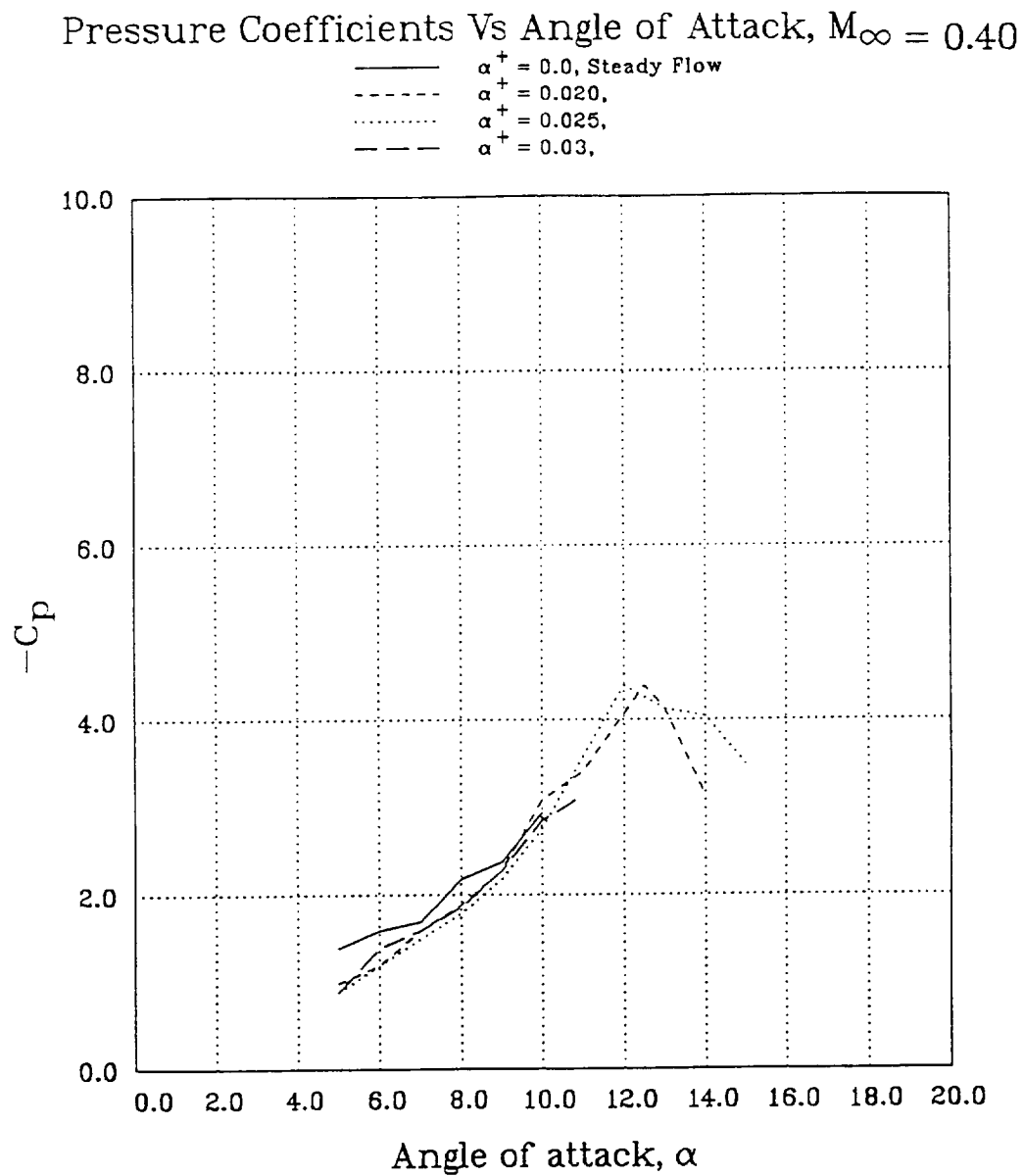|	
———	$\alpha^+ = 0.0$, Steady Flow
— — — — —	$\alpha^+ = 0.020$,
·················	$\alpha^+ = 0.025$,
— — —	$\alpha^+ = 0.03$,

Fig. 11. Effect of Pitch Rate on Peak Scution Pressure Coefficient, M = 0.4.
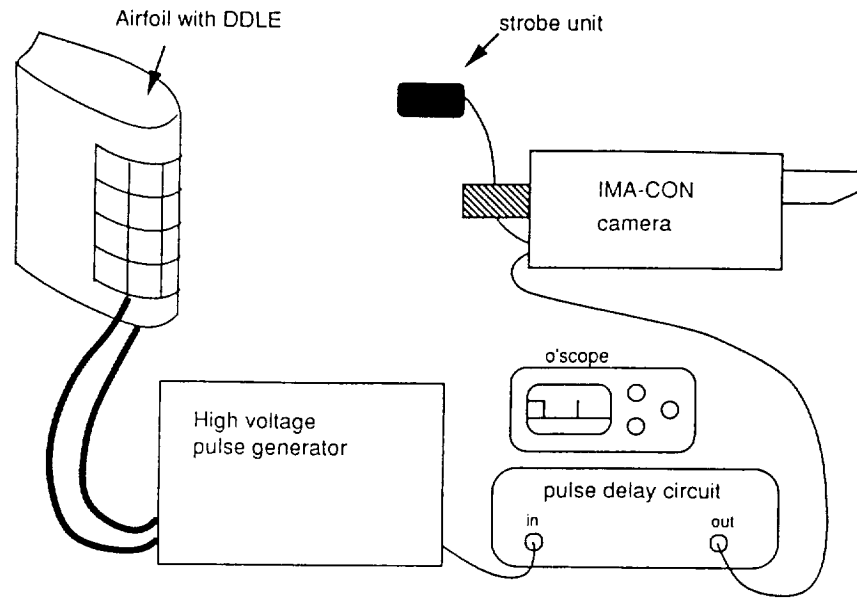
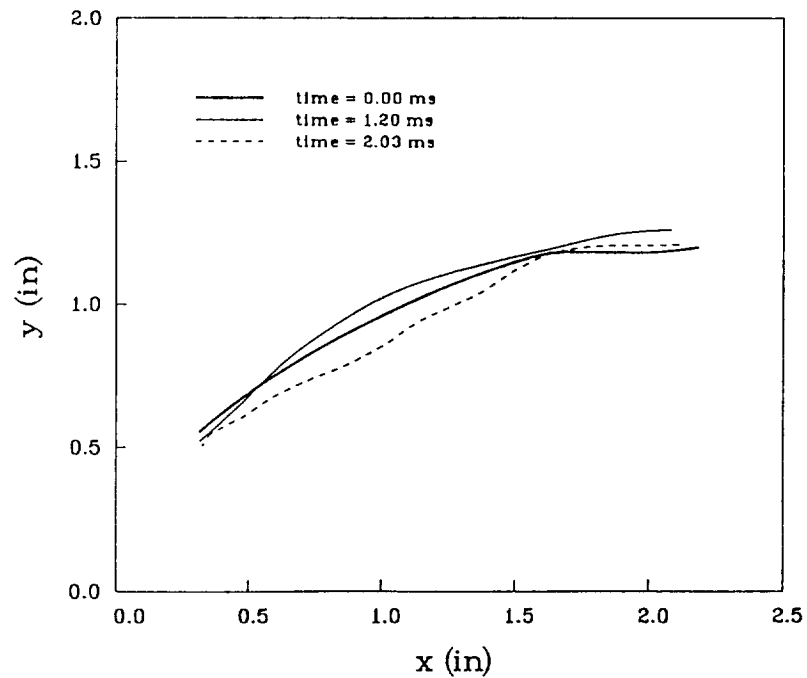Fig. 12. Schematic of the Dynamically Deforming Leading Edge Deflection Recording Method.

Fig. 13. DDLE Airfoil Contour at Midspan at Three Instants.

REPORT DOCUMENTATION PAGE

Form Approved
OMB No. 0704-0188

Public reporting burden for this collection of information is estimated to average 1 hour per response, including the time for reviewing instructions, searching existing data sources, gathering and maintaining the data needed, and completing and reviewing the collection of information. Send comments regarding this burden estimate or any other aspect of this collection of information, including suggestions for reducing this burden, to Washington Headquarters Services, Directorate for Information Operations and Reports, 1215 Jefferson Davis Highway, Suite 1204, Arlington, VA 22202-4302, and to the Office of Management and Budget, Paperwork Reduction Project (0704-0188), Washington, DC 20503.

1. AGENCY USE ONLY (Leave blank)	2. REPORT DATE Nov. 1992	3. REPORT TYPE AND DATES COVERED Final Report 10/89 - 09/92

4. TITLE AND SUBTITLE
Compressibility Effects on Dynamic Stall of Airfoils Undergoing Rapid Transient Pitching Motion

5. FUNDING NUMBERS
2307/CS
61102F

$IN-02-TM$

$\partial 352 7$

$28 P$

6. AUTHOR(S)
M.S. Chandrasekhara & M.F. Platzer

7. PERFORMING ORGANIZATION NAME(S) AND ADDRESS(ES)
Code AA/CH
Navy-NASA Joint Institute of Aeronautics
Department of Aeronautics and Astronautics
Naval Postgraduate School
Monterey, CA. 93943

8. PERFORMING ORGANIZATION REPORT NUMBER

9. SPONSORING/MONITORING AGENCY NAME(S) AND ADDRESS(ES)
U.S.Air Force Office of Scientific Research
Bolling AFB
Washington, D.C. 20332-6448

10. SPONSORING/MONITORING AGENCY REPORT NUMBER

11. SUPPLEMENTARY NOTES

12a. DISTRIBUTION/AVAILABILITY STATEMENT

Approved for public release; distribution unlimited.

12b. DISTRIBUTION CODE

13. ABSTRACT (Maximum 200 words)

The research was carried out in the Compressible Dynamic Stall Facility, CDSF, at the Fluid Mechanics Laboratory (FML) of NASA Ames Research Center. The facility can produce realistic nondimensional pitch rates experienced by fighter aircraft, which on model scale could be as high as 3600^0/sec. Nonintrusive optical techniques were used for the measurements. The highlight of the effort was the development of a new real time interferometry method known as Point Diffraction Interferometry - PDI, for use in unsteady separated flows. This can yield instantaneous flow density information (and hence pressure distributions in isentropic flows) over the airfoil. A key finding is that the dynamic stall vortex forms just as the airfoil leading edge separation bubble opens-up. A major result is the observation and quantification of multiple shocks over the airfoil near the leading edge. A quantitative analysis of the PDI images shows that pitching airfoils produce larger suction peaks than steady airfoils at the same Mach number prior to stall. The peak suction level reached just before stall develops is the same at all unsteady rates and decreases with increase in Mach number. The suction is lost once the dynamic stall vortex or vortical structure begins to convect. Bases on the knowledge gained from this preliminary analysis of the data, efforts to control dynamic stall were initiated. The focus of this work was to arrive at a dynamically changing leading edge shape that produces only 'acceptable' airfoil pressure distributions over a large angle of attack range.

14. SUBJECT TERMS
Dynamic stall, Unsteady Separation, Compressibility Effects, Interferometry, Control of Stall

15. NUMBER OF PAGES
27

16. PRICE CODE

17. SECURITY CLASSIFICATION OF REPORT	18. SECURITY CLASSIFICATION OF THIS PAGE	19. SECURITY CLASSIFICATION OF ABSTRACT	20. LIMITATION OF ABSTRACT
UNCLASSIFIED	UNCLASSIFIED	UNCLASSIFIED	UL

NSN 7540-01-280-5500

Standard Form 298 (Rev. 2-89)
Prescribed by ANSI Std. Z39-18